The Geometry and Electronic Topology of Higher-Order Charged Möbius Annulenes†

Chaitanya S. Wannere,‡,§ Henry S. Rzepa,*,⊥ B. Christopher Rinderspacher,‡,∥ Ankan Paul,‡,¶ Charlotte S. M. Allan,⊥ Henry F. Schaefer III,‡ and Paul v. R. Schleyer*,‡

Department of Chemistry and the Center for Computational Chemistry, University of Georgia, Athens, Georgia 30605, Department of Chemical Engineering, Stanford University, 381 North South Mall, Stanford, California 94305, and Department of Chemistry, Imperial College London, South Kensington Campus, Exhibition Road, London SW7 2AY, U.K.

Received: March 11, 2009; Revised Manuscript Received: June 8, 2009

Ⓦ This paper contains enhanced objects available on the Internet at http://pubs.acs.org/JPCA.

Higher-order aromatic charged Möbius-type annulenes have been $L_k$realized computationally. These charged species are based on strips with more than one electronic half-twist, as defined by their linking numbers. The B3LYP/6-311+G(d,p) optimized structures and properties of annulene rings with such multiple half-twists ($C_{12}H_{12}^{2+}$, $C_{12}H_{12}^{2-}$, $C_{14}H_{14}$, $C_{18}H_{18}^{2+}$, $C_{18}H_{18}^{2-}$, $C_{21}H_{21}^{+}$, $C_{24}H_{24}^{2-}$, $C_{28}H_{28}^{2+}$, and $C_{28}H_{28}^{2-}$) have the nearly equal C−C bond lengths, small dihedral angles around the circuits, stabilization energies, and nucleus-independent chemical shift values associated with aromaticity. The topology and nature of Möbius annulene systems are analyzed in terms of the torus curves defined by electron density functions ($\rho(r)_\pi$, ELF_π) constructed using only the occupied π-MOs. The π-torus subdivides into a torus knot for annulenes defined by an odd linking number ($L_k = 1, 3\pi$) and a torus link for those with an even linking number ($L_k = 2, 4\pi$). The torus topology is shown to map onto single canonical π-MOs only for even values of L_k. Incomplete and misleading descriptions of the topology of π-electronic Möbius systems with an odd number of half twists result when only signed orbital diagrams are considered, as is often done for the iconic single half twist system.

Introduction

Heilbronner's insightful 1964 paper, "Hückel Molecular Orbitals of Möbius-Type Conformations"[1] suggested "a closed shell configuration of an annulene with 4 p orbitals (r is any integer) can be twisted into a Möbius strip conformation without loss in π electron energy." This concise statement, which was based on a very simple theoretical analysis, spawned an interest in the chemistry of π-conjugated systems with Möbius properties that continues to grow and to diversify to the present day.[2]

The availability of several recent, extensive reviews[2a−c] obviates the need to recount all but the most pertinent historical and the more recent developments here. Heilbronner's examination of molecular models suggested that the torsional and angular strain inherent in Möbius systems might be overcome in larger annulenes. Indeed, the Möbius character present in *neutral half-twist* [20]-, [16]-, and the even smaller [12]annulenes has recently been established computationally.[3] Interest in Möbius aromaticity had already been rejuvenated in 1998 by the belated recognition of the Möbius π-aromatic character of the charged cyclic 8π electron $(CH)_9^+$ [9]annulene **1**.[4e,f] This cyclonona-2,4,6,8-tetraenyl cation had been generated independently in 1971 by Barborak, Su, Schleyer, Boche, and Schneider in solvolysis experiments and by Anastassiou and Yakali in ion stabilizing SO_2 solution, but its character was not fully recognized at that time.[4] In a remarkable 2003 accomplishment, Herges, et al. synthesized the first stable crystalline Möbius [16]annulene derivative[5] but whether this species is really aromatic is much debated.[3c,6] Castro, Karney, et al. invoked[7] a Möbius fully delocalized, aromatic transition state for the isomerization of tri-*trans*-[12]annulene to a di-*trans*-[12]annulene, and they[3d] and Warner[8] went on to develop the concept of Möbius antiaromaticity. Karney et al. showed that configurational change proceeding via twist-coupled bond shifting through a Möbius aromatic transition state is the most facile pathway in the [16]annulene automerization procees.[3e] In a recent study on [11]annulenium cations, Warner investigated and predicted the geometry of the first Möbius antiaromatic structure.[8] Metallacyclic systems with Möbius character have been identified recently;[9] many examples were shown to be aromatic on the basis of the nucleus-independent chemical shift (NICS)[10] as well as geometric and energetic criteria.

The consequences of higher-order twists imposed upon the p-AO basis of cyclic π-systems have been explored by chemists only lately.[11] Möbius himself was the first to consider strips with higher order twists, leaving in his unpublished papers[12] illustrations of those with not only one, but two and three half twists, and in recognition of this, we continue to refer to these also as (higher order) Möbius systems. The first reported annulene for which the p-AO basis (we now know) has the equivalent of a double twist in the π-system was a [16]annulene first described in 2000[3a] (although at the time, it was wrongly described as a single half-twist system). A neutral [12]annulene was reported by Castro, Karney, Schleyer, et. al in 2002, who described the most stable calculated isomer as having two half-twists, but manifested as a nonaromatic system with alternating

† Part of the "Walter Thiel Festschrift".

* To whom correspondence should be addressed. E-mail: h.rzepa@imperial.ac.uk, schleyer@chem.uga.edu.

‡ University of Georgia.

⊥ Imperial College London.

§ Current address: Forest Research Laboratories, 49 Mall Drive, Commack, NY, 11725.

∥ Current address: Dept. of Chemistry, Duke University, Box 97, Durham, NC 27705.

¶ Current address: Stanford University.

10.1021/jp902176a CCC: $40.75
Published on Web 07/28/2009

SCHEME 1: Illustration of the Schleyer-Pühlhofer ISE Method, Used to Compute an ASE of 2.8 kcal/mol for C_2 [10]Annulene

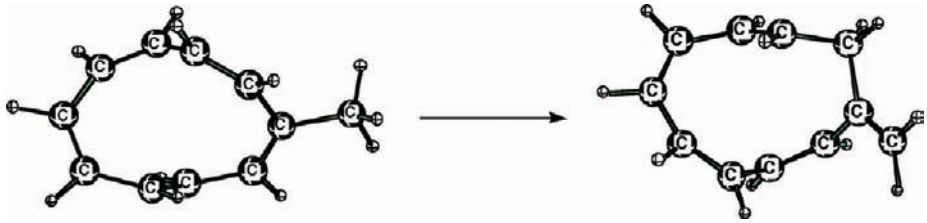

C−C bond lengths (Δ_r 0.103 Å).[3b] In 2006, Fowler and Rzepa formalized the π-electron selection rules for higher-twisted π-systems and were the first to speculate[13a] that a proportion of the electronic "twist" can be exchanged for a "writhe"[13b,c] in 3D space, with a consequent improvement in π overlap and energy. They cited the example of the twisted (and writhed) [14]annulene of D_2 symmetry, which had been noted in 2005[14] to exhibit almost no bond length alternation (Δ_r 0.012 Å) and to be competitive energetically with an untwisted Hückel conformation with C_s symmetry. This D_2 symmetric isomer has a "figure-eight" or lemniscular form, now recognized as characteristic of many systems with a double twist. The barrier to electrocyclic ring closure of (*Z*, *E*, *Z*)1,3,5,7,9-decapentaene via a transition structure (TS) having two half-twists was similarly calculated to be comparable to the conventional achiral $4n + 2$ electron Hückel TS barrier.[15] Gard, Reiter, and Stevenson reported[16] the involvement of a di-trans conformation of [12]annulene in the dehydrohalogenation of 1,2,5,6,9,10-hexabromocyclododecane. Most recently, a number of "figure-eight" or lemniscular double-twisted phyrins have been characterized crystallographically and by NMR, including examples identified as both aromatic and as antiaromatic.[17] The current record holder is a pentadecanuclear metallacycle exhibiting six half-twists.[18]

We now report that several new charged annulene systems with higher-order half-twists of 3 and 4 are also possible. These structures are aromatic on the basis of the computed aromatic stabilization energy (ASE), magnetic susceptibility anisotropies (χ_{aniso}), magnetic susceptibility exaltations (Λ),[19] and isotropic NICS values in the ring centers.[20] For comparison, we have included Rzepa's recently reported[14] [14]annulene (see Figure 4). Unless otherwise stated, the results discussed in the text were computed at the B3LYP/6-311+G(d,p) level. The ASEs were evaluated using the Schleyer−Pühlhofer (SP) isomerization stabilization energy (ISE) method, and the same species were employed to evaluate Λ values (see Scheme 1).[21] Warner was the first to apply various ASE schemes to charged singlet and triplet aromatic species and to Möbius structures. He employed various model equations to predict ASEs and compared the results obtained to Schleyer's indene−isoindene approach.[21c] He further showed that the choice of unbalanced equations leads to errors of ∼10 kcal/mol from the best predicted ASEs and that evaluation of Λ values was less variant to the choice of isomers used. However, we do not intend to employ this approach because the optimization of the aromatic and nonaromatic counterparts of **2**−**11** with "torsionally rigid" cyclopentadiene appendages led to significant changes in the annulene conformations, which no longer resembled those of the parent systems. On the basis of the equation in Scheme 1, positive ISE/ASE values denote stabilization and negative values destabilization. Likewise and for consistency with our earlier studies, positive values of Λ based in Scheme 1 denote diatropicity.[21b,c]

Results and Discussion

We first review several fundamental properties of Möbius topology, since the terminologies have often been used in the literature imprecisely or are incomplete. We introduce two subtle properties of a Möbius strip, crucial to our arguments, which have not been sufficiently articulated before. The ribbon shown in Figure 1 (essentially the one Heilbronner used in his seminal article, *but without signed AOs*) was constructed analytically using segments with finite widths and lengths, but having zero thickness. Such a ribbon, formed by imparting an overall half-twist prior to its cyclization, has a (instantaneous) C_2 axis of symmetry, which can bisect the resulting ribbon at precisely two locations. There are three ramifications:

(i) Crucially, at these bisection locations, points a and a′ are clearly equivalent by symmetry (Figure 1a), but points b and c are not (Figure 1b). However, this is only true if the a−a′ and b−c vectors have finite length. Any object placed along vector a−a′ will not be exactly equivalent (degenerate) with one placed along vector b−c.

(ii) A center line (shown in black in Figure 1), defined as running around the middle of the ribbon at the half-way point of each vector (a−a′, b−c, etc), is constrained to two dimensions. A Möbius strip of zero width reduces to just this circle. The twist will be distributed as local torsions between adjacent vectors on the surface of the strip, each rotating about the center line. These local torsions must by definition sum to π (i.e., a half-twist for this specific case).

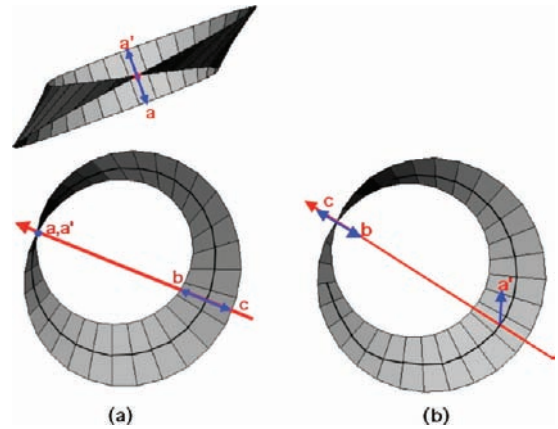

Figure 1. (a) Two perspective views of a segmented ribbon with single half-twist Möbius topology. The C_2 axis (red) bisects this ribbon at the midpoint of vector a−a′ (blue) and is concurrent with the axis of vector b−c (blue). Both vectors lie in the surface of the ribbon. Both a−a′ and b−c have (arbitrary) lengths, equal in this illustration to the width of the ribbon, and can be considered as representations of (unsigned) 2p AOs. A center line runs along the midpoints of the ribbon and is shown in black. (b) An alternative orientation, in which the vectors a′−a and b−c (blue) are now normal to the ribbon surface, with the C_2 axis again bisecting a−a′ and being concurrent with the axis of b−c.

(iii) In contrast, this is not true for ribbons whose center lines are *not* constrained to two dimensions. When these center lines encroach into three dimensions, the term *twist* acquires a subtly different meaning. The theorem introduced by White, Fuller, and Cãlugãreanu[22] summarizes the mathematical consequences of a three-dimensional ribbon:

$$L_k = T_w + W_r \quad (1)$$

As defined above, T_w refers to the sum of all local torsions; W_r (the writhe of the ribbon) is a nonlocal property reflecting the bending of the center line into three dimensions. Significantly, although both T_w and W_r may have fractional values, their sum (if expressed in appropriate units, see below) must be an integer. This sum is the linking number (L_k) of the ribbon. When a center line is constrained to two dimensions, $W_r = 0$; therefore, $L_k = T_w$ and our previous statement that a Möbius ribbon bears exactly, for example, one-half twist is, indeed, precise. We employed the term "twist" in the introduction (in quotation marks) because of its ubiquitous use in the literature, but we now emphasize that this usage is correct only for Möbius ribbons with exactly two-dimensional center lines. "Twist" must be carefully redefined for real three-dimensional molecules. In the following discussion, *twist* (italicized for clarity) refers specifically to T_w in eq 1. The previously accepted meaning of "twist" is now replaced by the concept of a linking number (L_k). In (nonchemical) contexts, L_k is conventionally given units of 2π and the term *integer* implies quanta of 2π. Because we will be dealing with the functional form of a p atomic orbital distributed along the center line of a ribbon, it is more convenient to assign units of π to L_k to assimilate the symmetry of such AOs. With this meaning, $L_k = 1$ (an integer) maps onto the now deprecated term "half-twist" and the expression "higher-order Möbius" now refers to systems with $L_k > 1$ values.

How does this terminology apply to Heilbronner's treatment of a cyclic annulene? Heilbronner distributed *unsigned and idealized* "p" atomic orbitals with local torsions evenly around the surface of a Möbius strip (of zero thickness). This is now defined as having linking number $L_k = 1(\pi)$. Heilbronner's (implicit) constraint of the center line of his Möbius strip to a 2D circle is exactly equivalent to placing the idealized p-AOs on a Möbius strip bearing one "half twist." His Hückel molecular orbital calculations on this model required pertinent approximations, the significance of which often has not been appreciated.

Heilbronner's p-AO basis was aligned with the node placed along the center line and with the orbitals oriented in the surface of the ribbon.[23] Two such AOs can be represented by the a−a′ or b−c vectors, noting that when the a−a′ AO is phased, it is antisymmetric with respect to the C_2 axis (i.e., of *b* symmetry), whereas b−c AO, phased or not, is symmetric with respect to this axis (i.e., of *a* symmetry).

The p-AO basis is defined for only one complete circuit of the ribbon. Because two complete circuits are required to return to the starting point of any proper Möbius strip with $L_k = 1$ (a result valid irrespective of whether the center line is constrained to 2D or 3D), following this AO basis for just one circuit must of necessity incur one phase shift (sign-inversion) in any (signed) LCAO combination constructed from this basis. This diagram of a single-circuit distribution of signed AOs around a Möbius strip is frequently used to illustrate the characteristics of Möbius molecules with one-half π-twist.[17b] However, such diagrams are misleadingly incomplete. Although a single circuit of AOs around the strip cannot return to the starting point without incurring a shift in the AO phases, there are, in fact, two more complete solutions to this problem that avoid such shifts/sign inversions, both of which are presented below.

The Hückel model carries no information regarding the width of the Möbius strip, which is implicitly zero. Fowler and Jenneskens[24] have stressed that although the total symmetry of a Möbius band is isomorphic with D_{oo}, an instantaneous "locked" C_2 symmetry is adopted by all reported molecular examples. The AOs, at the two intersections of this C_2 axis with the strip (Figure 1), can be degenerate/equal only for a Möbius strip of zero width. Consequently, the Hückel molecular orbital solutions for such zero-width systems misleadingly result in artificially degenerate pairs of π energy levels. For any real system, with Möbius strips having finite widths, degeneracy is always broken (the C_2 point group has no degenerate representations). One MO of this pair must have *b* symmetry with a nonzero coefficient for the AO located at a−a′ (Figure 1) and a zero value at b−c. The other MO of this pair will have *a* symmetry with a zero coefficient for the a−a′ AO. In many real cases, the energy splitting is not very large, and the erstwhile "degenerate" MO pair can be identified easily. Importantly, this quasi-degenerate pair provides the solution to the phase problem noted above; *both* MOs of such quasi-degenerate pairs, rather than one without the other, should be considered.

Heilbronner stated that he was not sure what the consequences of extending his two-dimensional model into three would be. We now recognize that the *twist* carried by the p-AO basis no longer needs be an integer multiple of π and that *writhe* must also be considered to describe the topology by an integer. The *linking number,* L_k, (the sum of the *twist* and the *writhe*) of the (unsigned) AO basis is the fundamental topological descriptor of the system. Any molecular orbital (singly or in combination) constructed from this basis by linear combination may or may not form a continuous surface (more formally, a torus) with an assignable linking number, but these MOs are a derived consequence of the basis set topology and do not fundamentally define it. In his own treatment, Heilbronner never illustrated signed MOs; neither did he refer to them as "Möbius orbitals" (the term Hückel in the title of his article referred to the method used to calculate their energies). Heilbronner's original unsigned p-AO depiction has been embellished with phases in later literature reports of his work. Such inaccurate depictions with C_2 symmetry are incompatible both with a Möbius strip, which must be unsigned, and with (pseudo)-degenerate MOs.

A further reality is that the MOs of real (three-dimensional) systems comprising a ring of carbon atoms resulting from any LCAO of the AO basis also undergoes mixing of the more complete 2s and 2p basis set AOs on each carbon. These no longer are precisely orthogonal and differ merely in energy. This hybridization can have the consequence that the phase shift (node), a mandatory requirement of a single cycle of a pure p-AO basis, may no longer be present in the set of real MOs, which are now only approximately described as π. Such σ/π mixing, however, of itself is not the fundamental cause for the breaking of the degenerate MO eigenvalues in the HMO treatment we noted above, although it certainly contributes.

Literature interpretations of Heilbronner's article have often couched their arguments in terms of π MO-twists, with the implication that these are capable of a unique and unambiguous definition of the topology of the system.[2] Cyclic ribbons that can sustain "twists" resulting in a computable linking number can be defined for two basic types of molecules. (1) True geometrically twisted systems are based on the nuclear geometry of the unmarked Möbius strip; cyclic DNA[25a] is an example of such, and Walba's molecular ladder is another.[25b] The ribbon

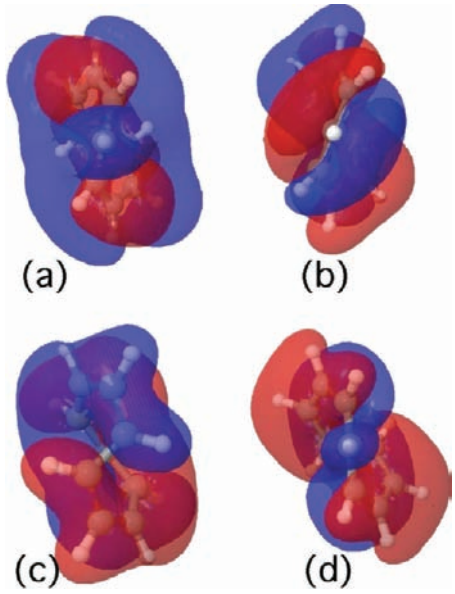

Figure 2. The four $\sim\pi$-MOs computed for $C_9H_9^+$ (**1**) comprising (a) the symmetric 30*a* and (b) antisymmetric 31*b* higher-energy pair and (c, d) the lower-energy pair 29*a* and 28*b*. Each "quasi-degenerate" pair corresponds to a degenerate energy level in the Heilbronner[1] HMO analysis. (See also the Web-enhanced table.)

is simply constructed from the coordinates of each atom defining the edge of the ladder. (2) Electronically "twisted" π-systems, the type we are discussing here, are based on the topological properties of a p-AO basis distributed with the node of each AO located on the center line of a ring of nuclei (two specific examples are illustrated as the vectors a−a′ and b−c in Figure 1). These vectors can be used to define a ribbon, which can be analyzed using eq 1.

Our use of the term "Möbius strip" requires specification. In molecular terms, it has in the past been taken to refer to a cyclic ribbon sustaining a single "half-twist". We now prefer to define it as a cyclic system for which the linking number, a topological property, can be computed and for which a p-AO (or in combination with a d-AO)[26] basis set is used to construct the ribbon used in this computation. Conventional Möbius systems have $L_k = 1$ (benzene has a $L_k = 0$ value), although as noted above,[12] Möbius himself considered strips with higher-order linking numbers (our terminology). Although linking numbers can also be negative (a pair of systems with, for example, $L_k = +1$ and -1 values may be enantiomers), we use only positive L_k values in the following discussion.

Annulenes with $L_k = 1$. The 8-π-electron $(CH)_9^+$ [9]annulene **1**[4] is an illustrative example. It has recently been formally demonstrated[27] to have $L_k = 1$, $T_w = 0.73$, and $W_r = 0.27\pi$ values, computed from the ribbon formed by a basis set of nine 2p-AOs distributed on each carbon of the ring. The projection of the center line connecting the nine nuclei into 3D space as writhe perturbs the system only modestly (hence, the "half-twisted" term is not an entirely unreasonable approximation). Four doubly occupied MOs resulting from a full SCF-MO treatment of the system are readily identified as having significant π character (Figure 2 and Web-enhanced table, which is available on-line in the HTML version of the paper). The two pairs, each of $a + b$ irreducible representations, correspond to the erstwhile degenerate pairs in Heilbronner−Hückel theory, but in reality, they are, of course, only "quasi-degenerate."

The degeneracy breaking (at the B3LYP/6-31G(d,p) level) is 0.0196 (0.53 eV) for the lower-energy pair and 0.0182 hartree (0.50 eV) for the higher-energy pair. The corresponding degeneracy-breaking values for the fully fluorinated system $(CF)_9^+$, 0.041 and 0.006 hartree, are much smaller. The lower C−F bond energy compared to a C−H σ-bond results in significantly less σ/π mixing in the fluorinated system. This decreases the energy separation, particularly of the lower-energy pair. Although the degeneracy breaking does not arise from σ/π mixing fundamentally, it does contribute to its magnitude.

The form of the MOs in Figure 2 also illustrates other points. The frame of reference of this real system has the C−H σ-framework embedded into the surface of the Möbius strip; the 2p-AO basis ribbon is orthogonal to this surface. As can be deduced from Figure 1b, the C−H and 2p-AO objects are oriented 90° to each other. Positions a + a′ and b + c are transposed with regard to those shown in Figure 1a, but they have the same properties. The most stable π-MO in this arrangement (28*b*) has a $p_\pi-p_\pi$ node at b−c and none at a−a′ (Figure 1b, when the AOs are signed); the slightly higher-energy MO of this pair (29*a*) is "reversed" because it has its $p_\pi-p_\pi$ node at a−a′ and none at b−c. This degeneracy breaking can be rationalized by arguing that a 2p-AO placed along b−c will have increased trans-annular repulsions, which are not compensated by improved overlap with adjacent 2p-AOs. Hence, the more stable MO avoids this, since a node is located at the same position. Because of their nodes, neither signed phase in 28*b* is cyclically continuous; this lack means that neither phase can be described as having Möbius character (in 3D terminology, neither phase forms a continuous torus). The symmetric partner 29*a* (of the quasi-degenerate pair, Figure 2d) is different in one significant regard: whereas one phase (red) has no torus form, the other phase (blue) actually exhibits one. However, this torus is completed only by virtue of participation from the C−H σ-bond lying along the C_2-axis. This $\sigma-\pi$ mixing is increased for the second-highest symmetric MO 30*a*, where each phase can adopt a torus form (Figure 2a). The two phases together form what is known as a "2_2 two-component torus link", for which L_k has the integer value of 2 rather than 1. Of the four π-like MOs for this $(CH)_9^+$ cation, only one (30*a*) can be described accurately as having Möbius character, and even this is weakened by its σ/π mixing and incorrect topology for a "half-twist" system!

If the $\sigma-\pi$ mixing perturbation is disregarded, no single canonical molecular orbital, derived from a π-annulene for which $L_k = 1$ and constructed from a pure 2p-AO basis, can have Möbius character. In effect, the LCAO coefficients describing a single MO can describe only a single circuit around the cycle. This is incomplete for a system with an odd value of L_k, for which two circuits are required to return to the starting point. Other functional transforms of the π-MOs are topologically more useful; for example, two-electron density descriptors.

The first such is the electron localization function (ELF),[28] which has also been proposed as a descriptor of π-aromaticity.[29] The ELF(r) function has value as a topological descriptor, because it can be computed from a subset of the occupied MOs;[30] for example, the four π-like MOs for **1** shown in Figure 2. The resulting ELF_π function has been contoured at four different isosurface values (Web-enhanced table). At the lowest value (0.25), this ELF_π function traces out a single continuous torus that makes two complete circuits of the ring. This type of single-component torus is formally known as a torus knot (although the "knot" in this case is trivial, being an "unknot", since it can be undone). This continuous function therefore satisfies the requirement for Möbius character in a system with $L_k = 1$. Although the ELF function actually was computed from all four occupied π-like MOs

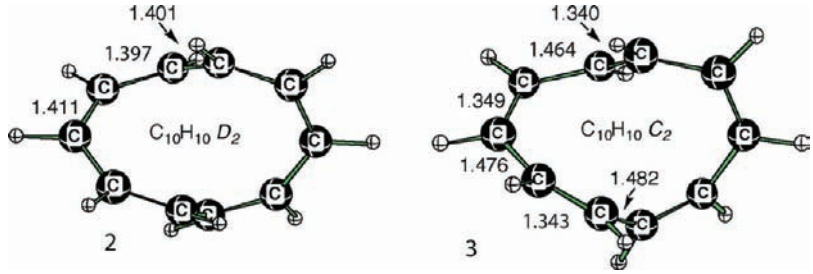

Figure 3. The B3LYP/6-311+G(d,p) optimized geometries of $C_{10}H_{10}$ with D_2 (**2**) and C_2 (**3**) symmetry.

for **1**, the minimal selection of MOs required to recover a similar ELF torus-knot topology is an occupied π-duo corresponding to just one Heilbronner degenerate pair (Web-enhanced table). An electron density transform of *two* appropriate π-MOs is the minimal requirement for recovering a formal Möbius topology for the electronic character of a system with $L_k = 1$ (a single half-twist) in the AO basis set topology. This requirement, when generalized, also holds for higher odd values of L_k (see below). Perturbation due to $\sigma-\pi$ mixing does not obscure this qualitative analysis, although it can result in the appearance of small "wormholes" connecting two or more regions of the π-torus (in this context, we define a wormhole as a shortcut or bridge analogous to the topological features of space−time which are valid solutions to the theory of general relativity).[31]

ELF_π thresholds for bifurcation of the continuous density function into so-called synaptic basins have been claimed[29] as providing an aromaticity index for planar aromatic species. High π-bifurcation values (~0.6−0.9, at which point the ELF_π function has separated into discrete valence basins) were taken to indicate high levels of aromaticity, whereas low π-bifurcation values (~0.25) were taken to indicate non- or antiaromaticity.[29] Although the major ELF_π bifurcation of **1** starts at ~0.33 (at the first crossing of the C_2 axis with the ring), the separation into π-valence synaptic basins is complete only at ~0.95. In view of this lack of a clear-cut single value for the bifurcation threshold, it seems that ELF_π can be used only as an approximate metric for Möbius aromaticity.

The electron density, $\rho(r)$, used in AIM topological analyses[32] is an even simpler function. When evaluated[30] for the π-MOs of **1** at an isosurface value of ~0.025 au, it reveals a topological interpretation qualitatively identical to the ELF_π function (Web-enhanced table), but with less contamination from the C−H σ-manifold and other artifacts. It is probably the function of choice for such topological analyses.

Annulenes with $L_k = 2$. The previous section illustrated how two complete circuits in a continuous electron density function such as ELF_π or $\rho(r)_\pi$ return a reference point back to its start in a Möbius cycle for which $L_k = 1$ (odd) without incurring a sign-inversion or node. A second mechanism also can accomplish this return. For systems with $L_k = 2$ (a double twist), only *one* complete circuit of the strip is required to return a function back to its starting point with no sign-inversion. This need not be an electron density function, but can also be a fully signed molecular orbital. Because a $L_k = 2$ system requires no mandatory sign inversion in any resulting MOs constructed from a 2p-AO basis, such MOs are capable of adopting a continuous toroidal Möbius form.[27] Where both single and double-half twist systems are discussed in the literature,[17] only the signed MO diagrams for the latter are correct topologically. The use of single signed MOs schematically for "half-twist" systems is incomplete topologically. We now discuss these statements by considering explicit examples of annulenes with $L_k = 2$.

The $C_{10}H_{10}$ conformation (**2**, D_2)[33] clearly is an example of such an annulene with $L_k = 2$ (Figure 3). Such systems exhibit a characteristic "figure eight" or lemniscular motif. The various possible conformations of [10]annulene were computed at several levels of theory by Schaefer et al. in 1999 in quest of predicting the energetically most preferred geometry.[33a] They had investigated the D_2 conformation of [10]annulene (**2**) and noticed that it is a transition state with a large imaginary vibrational frequency at the B3LYP and other DFT levels. Since [10]annulene is the smallest possible aromatic that can have $L_k = 2$, we have merely repeated a part of their work for comparison purposes here. Following the appropriate eigenvector leads to the C_2 geometry (**3**, Figure 3). However, **3** is also nonaromatic, as shown by its substantial bond alternation ($\Delta r = 0.142$) and a near zero isotropic NICS(0) value, Table 1. At the B3LYP/6-311+G(d,p) level, **2** is 11.4 kcal/mol higher in energy than **3**, whereas this difference increases to 18.4 kcal/mol at CCSD[T]/dzp//B3LYP/6-311+G(d,p). The nearly orthogonal HCCH dihedral angle (77.5°) along the $C_{10}H_{10}$ ring perimeter in **3** (ϕ in Table 1) eliminates effective π-overlap. Since the [10]annulene ring size is too small to accommodate lemniscular Möbius topologies satisfactorily, **3** is nonaromatic. We can add to the extensive previous discussion of this system by suggesting that this effect may also be interpreted in terms of the small size of the ring, which does not allow any significant proportion of the T_w component to be projected into W_r instead.[27]

Three additional annulene structures that can incorporate $L_k = 2$, $C_{12}H_{12}^{2+}$ (**4**), $C_{12}H_{12}^{2-}$ (**5**), and $C_{14}H_{14}$ (**6**) are shown in Figure 4. Due to its topology and resulting aromaticity (predicted recently by Rzepa),[14] **6** has been included here for comparison with the charged [12]annulenes, **4** and **5**. Moreover, we have extended the results on $C_{14}H_{14}$ by evaluating the ISE and Λ values. D_2 is the highest possible symmetry in these annulenes. As indicated in Table 1, these structures, indeed, are minima as characterized by a large, positive smallest frequency.

The B3LYP/6-311+G(d,p) optimized geometries displayed in Figure 4 show that the CC bond lengths in the annulenes are close to that in benzene (1.395 Å) [CC bond length in COT dianion and COT cation is 1.416 and 1.408 Å, respectively] and that the bond length alternations (Δr ranges from 0.011 to 0.027 Å, Table 1) along the ring perimeters are very small. The ASE values evaluated using the ISE method[21] are moderately large (12.1−16.1 kcal/mol, Table 1). The computed magnetic susceptibility exaltations are negative and larger (15.6−24.7 cgs.ppm) in magnitude than that of benzene (17.0 cgs.ppm). However, note that Λ values are dependent on the square of the ring area.[21b,34] The significantly negative isotropic NICS(0) values indicate that **4**, **5**, and **6** sustain diatropic ring currents and are aromatic. Note that the magnitudes of the ISE, isotropic NICS(0), and Λ values are proportional to the Δr values; thus, $C_{14}H_{14}$ (**6**), which shows the smallest CC bond alternation is more aromatic as compared to its isoelectronic $C_{12}H_{12}$ charged annulenes.

Lemniscular annulenes with a linking number of 2 are thus clearly viable. The computed CCSD[T]/dzp//B3LYP/6-311+G(d,p) energy of D_2 $C_{14}H_{14}$, **6**, is only 7.4 kcal/mol higher

TABLE 1: The Difference between the Shortest and Longest CC Bonds (Δr in Å), the Largest HCCH Dihedral Angle along the Annulene Ring Perimeter (ϕ in degrees), the Smallest Vibrational Frequency (ν in cm^{-1}), the Magnetic Susceptibility Anisotropies (χ_{aniso} in cgs.ppm), and the Total Isotropic NICS(0) (at the ring centers) of the Parent Annulenes; the Isomerization Stabilization Energies (ISE, kcal/mol) and Magnetic Susceptibility Exaltations (Λ, cgs.ppm), Evaluated Using the [*n*]Annulene Derivatives as in Scheme 1

		L_k[a]	Δ*r*[b]	ϕ[b]	ν[c]	ISE[f]	χ_{aniso}[d]	Λ[g]	NICS(0)[e]	digital repository[h] identifier[44]
C_6H_6	D_{6h}	0	0.000	0.0	414.9 (*E*)	34.6	−68.8	15.8	−8.8	10042/to-841
3	C_2	2	0.142	77.5	138.7	2.8 (2.6)	−12.5	−1.5	−1.4	10042/to-839
4	D_2	2	0.027	30.7	115.1	12.1 (11.5)	−61.9	15.6	−8.6	10042/to-835
5	D_2	2	0.019	23.3	106.8	14.3 (14.1)	−84.3	19.6	−17.4	10042/to-836
6	D_2	2	0.011	20.3	88.9	16.1 (16.1)	−59.2	24.7	−19.5	10042/to-837
7	D_3	3	0.018	25.8	71.2 (*E*)	9.9 (8.7)	−194.9	38.9	−10.9	10042/to-840
8	D_3	3	0.016	22.9	77.9 (*E*)	9.1 (8.2)	−172.2	49.6	−14.6	10042/to-848
9	D_3	3	0.007	16.5	65.0 (*E*)	14.7 (14.4)	−153.0	55.5	−13.8	10042/to-849
10	D_2	4	0.015	23.9	30.4	16.4 (16.1)	−276.9	89.7	−17.2	10042/to-842
11	D_2	4	0.008	21.4	28.1	15.1 (14.7)	−253.5	113.1	−15.1	10042/to-843
12	D_4	4	0.010	20.3	33.3	11.8 (11.1)	−322.8	129.7	−16.1	10042/to-844

[a] L_k represents the linking number. [b] Δr and ϕ computed at the B3LYP/6-311+G(d,p). [c] ν computed at the B3LYP/6-31+G*. [d] χ_{aniso} is the anisotropy computed at the CSGT-B3LYP/6-31+G*. [e] The isotropic NICS(0) values were evaluated in the ring centers of the parent annulenes using the deMon-Master NMR program, at SOS-DFPT level with the Perdew−Wang-91(PW91) exchange correlation functional and the IGLO-III TZ2P basis set using the B3LYP/6-311+G(d,p) geometry. [f] ISE is the aromatic stabilization energy computed at the B3LYP/6-31G* + ZPE (at B3LYP/6-31G*) using the Schleyer-Pühlhofer method (Scheme 1). The values in parentheses are ISEs with the zero point energy vibrational correction (B3LYP/6-31G*). [g] Λ is the magnetic susceptibility exaltation computed at the CSGT-B3LYP/6-31+G*//B3LYP/6-31G* using the ISE equations. [h] The identifier can be resolved as, for example, http://dx.doi.org/10042/to-837.

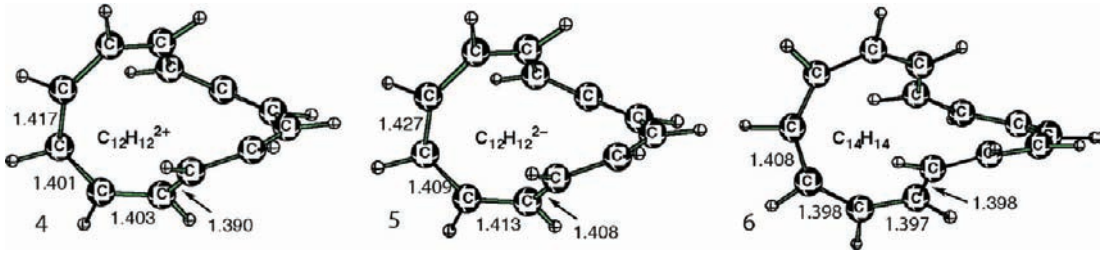

Figure 4. The B3LYP/6-311+G(d,p) optimized geometry of $C_{12}H_{12}^{2+}$ (**4**), $C_{12}H_{12}^{2-}$ (**5**), and $C_{14}H_{14}$ (**6**). All these annulenes have D_2 symmetry.

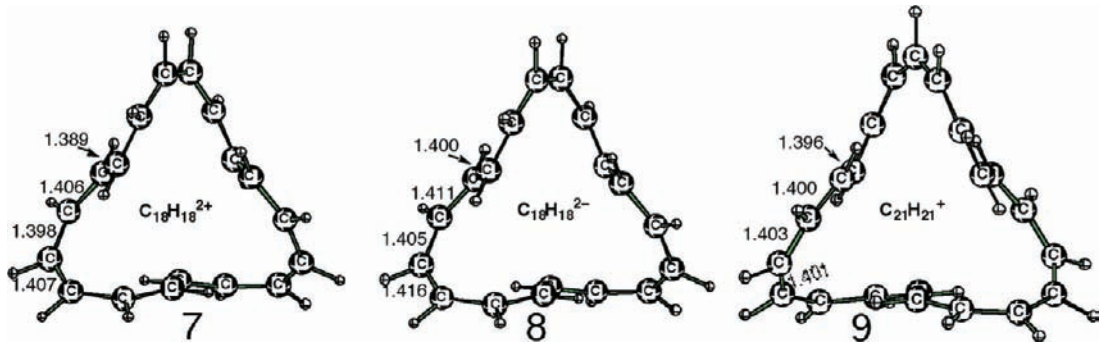

Figure 5. The B3LYP/6-311+G(d,p) optimized geometry of $C_{18}H_{18}^{2+}$ (**7**), $C_{18}H_{18}^{2-}$ (**8**), and $C_{21}H_{21}^{+}$ (**9**) annulenes in D_3 symmetry. The largest deviation from either 0° or 180° for CCCC torsions in these structures is, respectively, 37, 25, and 20°.

than that of the C_s $C_{14}H_{14}$ annulene, known to be almost planar from X-ray[35] analysis and computations.[36] The D_2 geometry becomes favored by substituting the inner four hydrogens of C_s $C_{14}H_{14}$ with more bulky fluorine atoms.[14]

Annulenes with $L_k = 3$. The topologies of $C_{18}H_{18}^{2+}$ (**7**), $C_{18}H_{18}^{2-}$ (**8**), and $C_{21}H_{21}^{+}$ (**9**) displayed in Figure 5 clearly demonstrate that annulenes with $L_k = 3$ and having D_3 symmetry are also possible (the value of $L_k = n$ maps nicely onto the D_n symmetries, being the highest possible for these systems). All three are true minima, with only positive vibrational frequencies (Table 1). The CC distances (Figure 5) are near 1.40 Å and exhibit very little bond alternation (the Δ*r*'s range from only 0.007 to 0.018 Å, Table 1). Furthermore, the small HCCH dihedral angles (ϕ in Table 1) permit effective π-overlap. The computed aromatic stabilization energy (ISE in Table 1) for **9** is 14.7 kcal/mol, but the ISEs of **7** and **8** are more modest in magnitude. The ISE of [18]annulene (27.4 kcal/mol)[21b] is 3 times as large as that of $C_{18}H_{18}^{2+}$ **7** (9.9 kcal/mol) and $C_{18}H_{18}^{2-}$ **8** (9.1 kcal/mol). The computed magnetic anisotropies and Λ values indicate diatropic ring currents in **7**, **8**, and **9**. In addition, the large and negative are the NICS(0) values (ranging from −10.9 to −14.6) in the geometric center of the heavy atoms, which characterizes these annulenes as aromatic. Although NICS(0) values for smaller ring systems can be misleading due to local effects (as noted previously,[3b] the "double-twisted" [10]annulene NICS(0) = 8.1 ppm at the centroid was attributed to the local effects of inwardly pointing π-bonds), these local effects attenuate rapidly for the larger **7**−**12** rings so that their NICS(0) values are likely to be reliable π indicators. Taken together with the small Δ*r* values and the energetic and the

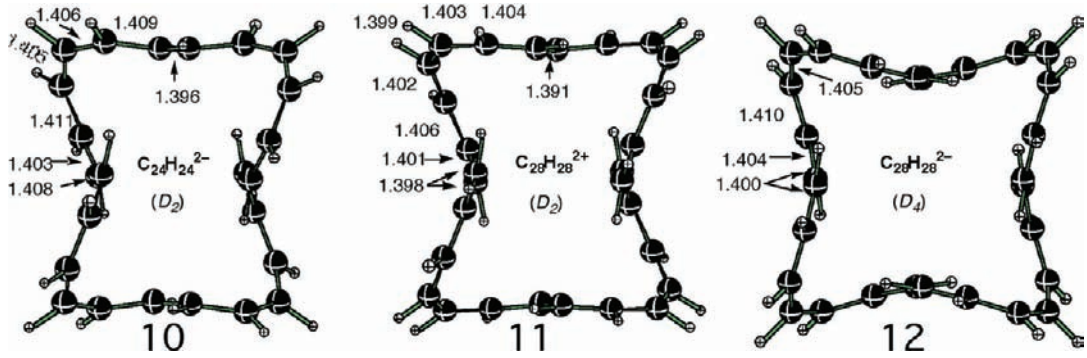

Figure 6. The B3LYP/6-311+G(d,p) optimized geometry of $C_{24}H_{24}^{2-}$ (**10**), $C_{28}H_{28}^{2+}$ (**11**), and $C_{28}H_{28}^{2-}$annulenes (**12**). The largest deviation from either 0° or 180° for CCCC torsions in these structures is, respectively, 34, 28, and 27°.

magnetic criteria, the calculations suggest that $C_{21}H_{21}^{+}$ **9** is the most aromatic among the three structures shown in Figure 5.

Annulenes with $L_k = 4$. As depicted in Figure 6, the topology of $C_{24}H_{24}^{2-}$ (**10**), $C_{28}H_{28}^{2+}$ (**11**), and $C_{28}H_{28}^{2-}$ (**12**) annulenes feature a linking number of 4. Although **12** adopts the highest possible D_4 symmetry, **10** and **11** prefer lower symmetry D_2 geometries. The nearly equal CC bond distances (small Δr) of the structures displayed in Figure 5 satisfy the geometric aromaticity criterion. The small dihedral angles in these Möbius annulenes show that the π-orbitals have favorable overlap around the ring perimeter. Moreover, the aromatic stabilization energies (from 11.8 to 16.4 kcal/mol, Table 1) are in the same range as those of the Möbius annulenes with $L_k = 2$, 3. The computed magnetic anisotropies and the Λ-values (from 89.7 to 129.7 cgs. ppm) show that **10**, **11**, and **12** annulenes are aromatic. The isotropic NICS(0) values (−15.1 to −17.2 ppm, Table 1) computed in the ring centers for these annulenes are much larger than that of benzene (−8.8). Thus, the geometric, energetic, and magnetic aromaticity criteria show that the $C_{24}H_{24}^{2-}$, $C_{28}H_{28}^{2+}$, and $C_{28}H_{28}^{2-}$ annulenes with $L_k = 4$ have significant diatropic character. Note that the ISE of $C_{28}H_{28}^{2-}$ (11.8 kcal/mol) is ~3.5 kcal/mol smaller than that of the other two systems, but this is in part due to the change in the topology of the nonaromatic reference isomer upon optimization. To overcome this problem of conformational change, the ISE was evaluated using the partially optimized structures of the aromatic and its nonaromatic counterpart by fixing their CCCC-dihedral angles to values like those of the optimized parent $C_{28}H_{28}^{2-}$ geometries.

Effects of Bond Alternation on Geometries. Some computed geometrical features of Hückel annulenes are known to depend on the level of theory.[33,36,37] For example, the B3LYP hybrid functional tends to predict delocalized, bond length-equalized structures, whereas the KMLYP hybrid optimizes to CC bond-alternating geometries.[36] Consequently, the structures of **2**−**12** also were optimized at the KMLYP/6-31G(d) level to ascertain the effects on the geometries. Both B3LYP and KMLYP predict highly delocalized geometries with similar CC bond lengths for **2**−**6** and **8** (see digital repository entries associated with Table 1). However, **7** and **9**−**12** prefer lower symmetry geometries with notable bond alternation when optimized at KMLYP. Structure **12** favors D_2 symmetry, whereas **7**, **9**, **10**, and **11** optimize to C_1 symmetry. The largest changes in geometry are found for the KMLYP-optimized **10** and **11**. The large values of the HCCH dihedral angles (ϕ close to 90°) in **10** and **11** virtually exclude π-overlap as well as aromaticity. Although **12** optimizes to D_2 symmetry, its aromatic character is retained with modest CC bond alternation (0.067 Å) along the ring perimeter and the large and negative NICS(0) value of −10.2 ppm in the center. At KMLYP/6-311+G(d,p), the D_4 symmetric form of **11** is only 0.9 kcal/mol higher in energy than the D_2 geometry. Due to its larger HF character, the KMLYP functional is more biased toward localized geometries; conversely, B3LYP may be biased toward delocalized geometries. Rzepa and Sanderson noted[37] that geometries intermediate between those predicted by B3LYP and KMLYP methods were closer to the X-ray structures of 10 electron π rings. In contrast, Herges et al. recently concluded[3c] that B3LYP (rather than KMLYP) bond lengths for Möbius structures are in better agreement with X-ray values. Whereas CCSD(T) geometries may be the most accurate,[37] structures **2**−**12** are too large to be characterized as minima by frequency computations at this level. The correct prediction of the onset of bond length alternation in Möbius annulene systems is a nontrivial issue, as the recent reanalysis of the structure of [18]annulene indicates.[36] Analysis of the reported[17a] crystal structures of the lemniscular ($L_k = 2$) systems **13** and **14**, revealed[17c] them as, respectively, [28] and [26]-π-electron antiaromatic and aromatic systems. Pairs of meso bonds from the carbon carrying the X substituent differ in the crystal structure, on average, by Δr ~0.079 and 0.015 Å for the antiaromatic and aromatic systems, respectively, the former revealing significant bond alternation, and the latter, little. The B3LYP and KMLYP values (X = CF_3, 6-311+(d,p) basis) differ by 0.065 and 0.081, respectively, for **13** and by 0.003 and 0.006 Å, respectively, for **14**. Thus, for helical molecules of the type **2**−**12**, both B3LYP and KMLYP can reproduce a lack of bond alternation in the region of a cyclic 26/4n+2 π-electron system, calibrated against a system (**13**) that does show such bond alternation.

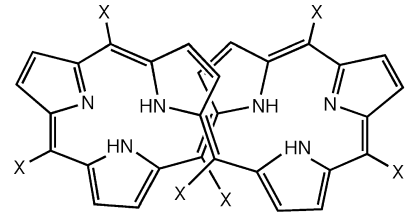

13, X=CF_3

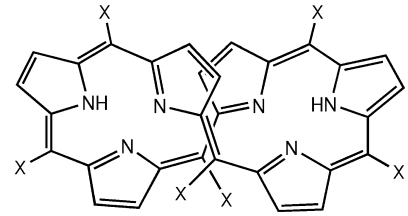

14, X=CF_3

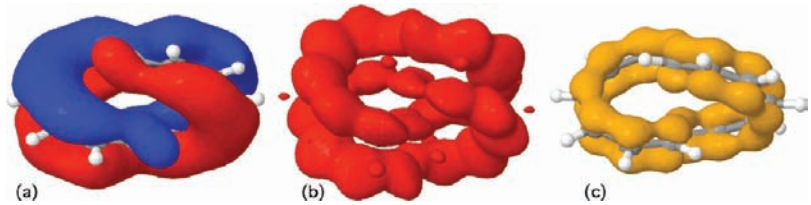

Figure 7. (a) The π-MO ($44B_2$) for **6** corresponding to a continuous torus curve. (b) ELF_π isosurface summed over all seven occupied π-MOs and contoured at 0.40. (c) $\rho(r)_\pi$ electron density, summed over all seven occupied π-MOs and contoured at 0.024 au. All three torus curves take the form of a torus link (cf. Figure 8b). (See also the Web-enhanced table.)

The threshold for the appearance of bond alternation and the best method to predict it remain open problems. Reddy and Anand's[38] recent X-ray structure of **15**, regarded as a [30]-π-electron macrocycle (i.e., the same electron count as **12**) might have been instructive, but the crystallographic refinement (R = 7.2%) was not sufficiently precise to provide a clear answer.[39]

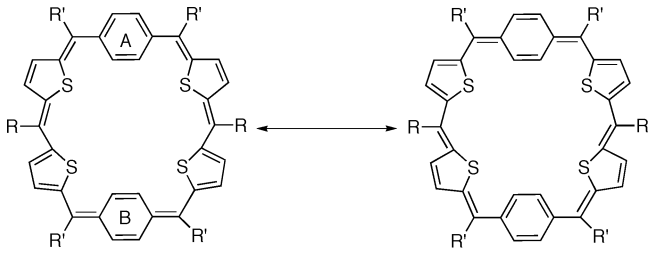

15, R=$C_6H_3F_2$, R'=C_6F_6

Topological Classification. We argue that topological electronic analysis in terms of (signed) linking numbers is a useful and more general extension of the hitherto accepted procedures, such as noting the odd/even number of transoid units present in the ring[7] or counting the minimum number of sign inversions manifest in the p-AO basis set.[1,2e,f] Whereas the latter is an unsigned property that can have only two reduced values (0 or 1) and which does not therefore formally distinguish between, for example, untwisted and doubly twisted cycles, or between, for example, singly and triply twisted annulenes, linking numbers provide such cycles with a more specific description of any order of "twist." Because the linking number is signed, it can also be used to designate absolute chirality, as can the signed values of T_w and W_r intrinsic to this concept. The linking number is more applicable for analyzing not only more complex ring systems such as **13**−**15** but also deceptively simpler systems such as the Möbius conformation of azepine,[40] which has no transoid motif or clear-cut sign inversion.[31] Finally, we note that linking numbers can also be used to classify electron density torus curves, where the concept of a sign inversion cannot occur (the density, of course, being related to the square of the AO coefficient).

Heilbronner HMO theory[1] predicts (pseudo)-degenerate π-energy levels for the base Möbius system (L_k = 1 and, more generally, for all odd values of L_k), from which, of course, the $4n$-electron occupancy rule for singlet stability has been derived. When the same approach is applied[13] to systems with L_k = 2 (and more generally, for all even values of L_k), the energy levels now follow the pattern obtained for benzene itself. For neutral systems, a single nondegenerate level is the most stable, followed by degenerate occupied pairs, and from which a $4n$ + 2 electron occupancy rule for singlet stability can be derived. However, none of the structures **2**−**6**, **10**−**11** actually have degenerate orbitals at the different levels of theory investigated (the D_2 group has no degenerate representations, although D_3 and higher D_n groups do). As already noted, even a small Möbius system such as **1** does not follow the simple Heilbronner HMO derivation; the π MOs are only pseudo-degenerate. As discussed above, this artifact in simple HMO theory is due to the finite width of the Möbius ribbon, with a further perturbation due to 2p−2s AO mixing, the extent of which varies along the ring perimeter and with the size of the system.

However, the systems with even linking numbers are fundamentally different from the odd-numbered series in that only a single circuit of the ring is needed to return to the starting point (in this sense, even values of L_k map onto orbital ribbons with zero sign inversions, and odd values of L_k map onto those with one sign inversion). Consequently, topologies with an even linking number *can* be represented by a single (nondegenerate) π-MO. This is illustrated for **6** (Web-enhanced table and Figure 7). Of the required seven doubly occupied π-levels, orbital 44 (the B_2 symmetric second π-level) has the form of a figure eight or a lemniscus, and both (signed) phases are clearly continuous around the circuit. This type of 3D form is known as a torus link (because the two phases are linked and inseparable). The next orbitals, 43−41, are purely σ in origin, and the final occupied π-type orbital occurs only at level 40. This again is a departure from the Heilbronner HMO benzeneoid model. That σ−π mixing is primarily responsible was demonstrated by perfluorination of the rin.[14] Due to the σ withdrawing F effect, the continuous lemniscular π-orbital becomes the lowest on the π-manifold. The ELF_π and $\rho(r)_\pi$ functions computed purely from these seven occupied π-orbitals match orbital 40 for compound **6** exactly in its topology (Web-enhanced table), taking the form of a two-component torus link. Mathematically idealized versions of such torus curves are shown in Figure 8 for comparison with the curves computed for **6** (Figure 7).

We have verified that the topology of the π MOs does not depend on the level of theory (AM1, HF/3-21G*, HF/6-31G(d), HF/6-31+G(d), HF/6-311+G(d,p), B3LYP/6-31G(d), KMLYP/6-31G(d), and MPW1PW91/6-31G(d)) computed using the //B3LYP/6-311+G(d,p) geometry. Hence, the inferred topology from the ELF_π or $\rho(r)_\pi$ functions also does not depend on HF or density functional or the size of the basis set.

We next consider systems **7**−**9** with an odd value of 3 for the linking number, and two with higher odd values of L_k = 5, 7 (Web-enhanced table). These were all computed for (idealized) D_n symmetries, n = 3, 5, 7. These point groups *do* have degenerate (E) irreducible representations; consequently, exactly degenerate MO energy levels are found (one each of the lowest energy pair for L_k = 3, 5, 7 is illustrated in the Web-enhanced table). As for L_k = 1, a single circuit around the cycle must lead to a phase shift or sign inversion (again, assuming no σ−π mixing), and again, no *single* MO for such odd L_k valued systems can form a torus knot with Möbius character. However, as with L_k = 1, the ELF_π and $\rho(r)_\pi$ functions computed from just the occupied π-MOs *do* have this character, forming continuous torus knots (rather than links) designated n_1, where

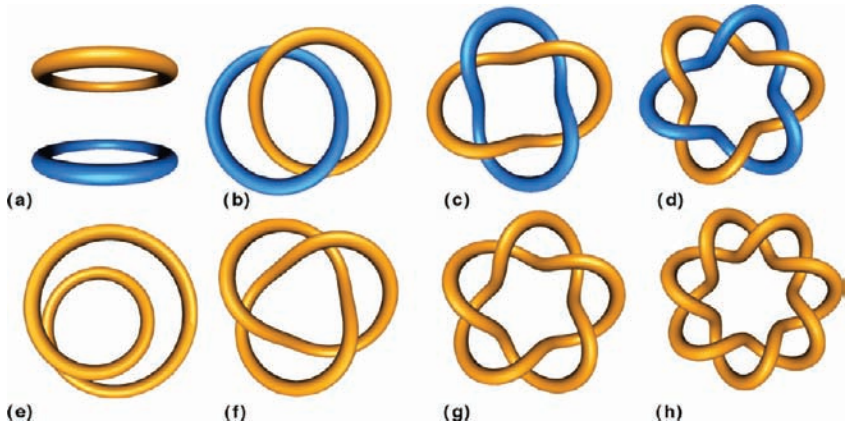

Figure 8. Torus links, defined by linking numbers L_k (a) 0, (b) 2, (c) 4 (d) 6 (in units of π). Torus knots, defined by L_k (e) 1, (f) 3, (g) 5, and (h) 7. Diagrams were generated using Knotplot, http://knotplot.com/. (See also the Web-enhanced table.)

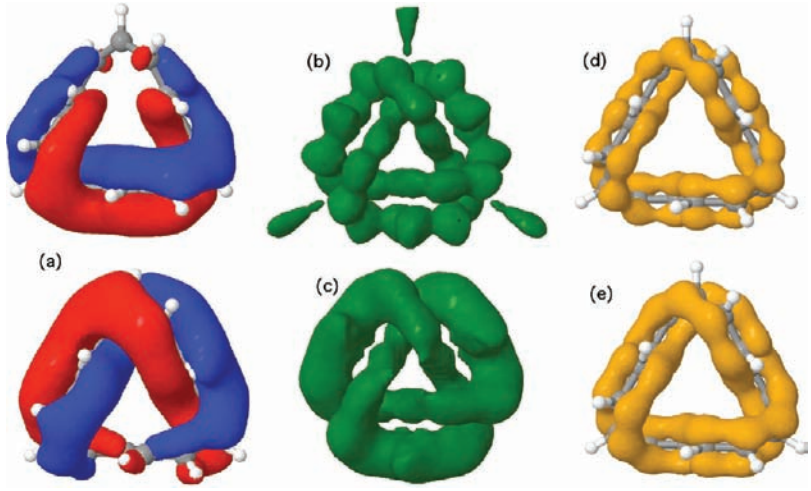

Figure 9. (a) Lowest-energy degenerate π-MO (46/47E) for D_3-symmetric $C_{15}H_{15}^-$, each MO revealing a phase shift (node) in the function. (b) ELF_π isosurface contoured at 0.40, summed over all eight occupied π-MOs. (c) ELF_π isosurface contoured at 0.40, summed over 46/47E π-MOs only. (d) $\rho(r)_\pi$ electron density, summed over all eight occupied π-MOs. (e) $\rho(r)_\pi$ electron density, summed over 46/47E π-MOs only. (b−e) These take the form of a trefoil knot (c.f. Figure 8f). (See also the Web-enhanced table.)

$n = 3, 5, 7$, etc., and none of which resemble an individual MO. The torus knot derived for $L_k = 3$ adopts a precise trefoil form (Figure 9).

In summary, topological analysis of the π-electron density of the classical Heilbronner Möbius $C_9H_9^+$ annulene cation (**1**) reveals that the pure p-AO basis can be used to construct a function, which completes two formal circuits around the ribbon in which the basis set is embedded. A characteristic three-dimensional topological form known as a torus knot results. The analysis can be generalized by the more general linking number L_k of this torus, rather than by the extent of a "half-twist" or presence of an AO sign-inversion. It follows that any electronic Möbius annulene whose p-AO basis is defined by an *odd* linking number can result in a π-electron density function in the form of a torus knot, encircling the cycle exactly twice. No individual molecular orbital derived from a pure 2p AO basis can reflect this topology, but perturbation by $\sigma-\pi$ mixing can result in a single MO for an odd L_k system having the (misleading) appearance of a continuous torus link. The corollary is that any electronic Möbius annulene for which the p-AO basis ribbon is defined by an *even* linking number can result in an electron density function taking the form of a two-component torus link; each component of this torus circles the cycle exactly once. It is possible (although not necessary) for a single molecular orbital in such even L_k systems to display the same topological form.

Conclusions

The ability of annulenes to undergo both one- and two-electron oxidations and reductions to produce a variety of charged species with interesting aromatic properties has been recognized for some time.[41] Whereas this previous focus was predominantly on effectively planar achiral systems, here we have extended the scope to an analysis of the geometries and aromatic features of a range of hypothetical charged annulenes that exhibit more complex twisted topologies associated with chiral rather than achiral properties. Hoffmann, Schleyer, and Schaefer in their article "Predicting Molecules− More Realism, Please" have recommended that prediction of new molecules and of their stability should also be accompanied by the computation of barriers to rearranged products or conformations.[42] As was, indeed, originally recognized by Heilbronner,[1] a full conformation exploration for larger annulenes still constitutes a major challenge. Moreover, there is existing experimental evidence that shows the tendency of annulenes to easily undergo rearrangement and automerization, even under ambient conditions.[43] At this stage, we nevertheless note that the computed large lowest vibrational frequencies and the HOMO−LUMO gap of our systems provide encouragement that they might serve as further inspiration for experimental realization.[17]

Here, our focus is also on the Möbius topological features of such systems. Since Heilbronner's[1] introduction of the concept of Möbius π-electronic systems, it has become common to illustrate (if only schematically) the topology of such systems using a (signed) cyclic single circuit of 2p-AOs. It is implied that such diagrams convey the essential characteristics of the Möbius strip appropriately. They do not. These representations with differentiated p-AO lobes are discontinuous, because they must have a sign inversion. This violates the requirements that Möbius systems be cyclic, nonorientable, and have a single-sided surface. The more recent discovery of many real molecules exhibiting such features, and the extension to higher order twists, emphasizes the need for a more general methodology for the topological analysis of such systems. Our proposal involves analysis of the topology of the π-electron density function of Möbius molecules, rather than using single signed molecular orbitals derived from 2p-AOs. We recommend the use of linking numbers, L_k, which refer to the form of the torus curve defined by the π-electron density function, to replace the looser "half-twist" term to describe these systems. The π-density of systems with an odd value n for L_k is described by a continuous torus knot, which doubly encircles the ring, crossing over itself n times during this circuit. The π-density of systems where n is even takes the form of a torus link with two components, which cross over each other n times, each encircling the ring once. A number of higher-order Möbius annulenes that illustrate these properties are revealed as dissymmetric/chiral minima having highly aromatic characteristics.

Acknowledgment. We dedicate this paper to Walter Thiel in appreciation of his seminal contributions to the development of computational chemistry methodology. This work was supported by PRF Grant 41888-AC4 and by NSF Grants CHE-0209857 and 0716718. We thank Michael Mauksch for his interest and comments.

Supporting Information Available: Full information for the systems reported in Table 1 and the Web-enhanced table are available via the links to the digital repository. The function of this repository is explained in ref 44. This material is available free of charge via the Internet at http://pubs.acs.org.

References and Notes

(1) Heilbronner, E. *Tetrahedron Lett.* **1964**, 1923–1928.

(2) For reviews on Möbius aromaticity, see: (a) Rzepa, H. S. *Chem. Rev.* **2005**, *105*, 3697–3715. (b) Kawase, T.; Oda, M. *Angew. Chem., Int. Ed.* **2004**, *43*, 4396–4398. (c) Herges, R. *Chem. Rev.* **2006**, *106*, 4820–4842. (d) Zimmerman employed a Möbius concept of sign inversions in the p-AO ribbon to deduce the allowed processes for a variety of electrocyclic reactions and generalized Hückel-Möbius selection rules. Zimmerman, H. E. *J. Am. Chem. Soc.* **1966**, *88*, 1564–1565. (e) Zimmerman, H. E. *Acc. Chem. Res.* **1972**, *4*, 272–280. Indeed, energetic and magnetic criteria confirm that the Hückel ($4n + 2$)-electron and Möbius ($4n$)-electron transition states of several pericyclic reactions are aromatic. (f) Jiao, H.; Schleyer, P. v. R. *Angew. Chem., Int. Ed.* **1993**, *32*, 1763–1765. (g) Jiao, H.; Schleyer, P. v. R. *J. Chem. Soc., Perkin Trans. 2,* **1994**, *40*, 7–410. (h) Herges, R.; Jiao, H.; von Ragué Schleyer, P. *Angew. Chem., Int. Ed.* **1994**, *33*, 1376–1378. (i) Cossio, F. P.; Morao, I.; Jiao, H. J.; Schleyer, P. v. R. *J. Am. Chem. Soc.* **1999**, *121*, 6737–6746. (j) Tokuji, S.; Shin, J.; Kim, K.; Lim, J. M.; Youfu, K.; Saito, S.; Kim, D.; Osuka, A. *J. Am. Chem. Soc.* **2009**, *131*, 7240–7241.

(3) (a) Martín-Santamaría, S.; Lavan, B.; Rzepa, H. S. *J. Chem. Soc. Perkin Trans 2,* **2000**, 1415–1417. Analysis of the p-orbital ribbon for the [16]annulene reported in this article has now revealed the following values: $L_k = 2$, $T_w = 1.73$, $W_r = 0.27$p. Systems with even values of L_k and $4n$-electron counts cannot be aromatic, and in reality, they most likely adopt nonaromatic geometries. (b) Castro, C.; Isborn, C. M.; Karney, W. L.; Mauksch, M.; von Ragué Schleyer, P. *Org. Lett.* **2002**, *4*, 3431–3434. (c) Ajami, D.; Hess, K.; Köhler, F.; Näther, C.; Oeckler, O.; Simon, A.; Yamamoto, C.; Okamoto, Y.; Herges, R. *Chem.—Eur. J.* **2006**, *12*, 5434–5445. (d) Moll, J. F.; Pemberton, R. P.; Gutierrez, M. G.; Castro, C.; Karney, W. L. *J. Am. Chem. Soc.;* **2007**, *129*, 274–275. (e) Pemberton, R. P.; McShane, C. M.; Castro, C.; Karney, W. L. *J. Am. Chem. Soc.* **2006**, *128*, 16692–16700. (f) Mauksch, M.; Tsogoeva, S. B. *Angew. Chem. Int. Ed.* **2009**, *48*, 2959–2963.

(4) (a) Barborak,; J, C.; Su, T. M.; Schleyer, P. v. R.; Boche, G.; Schneider, J. *J. Am. Chem. Soc.* **1971**, *93*, 279–281. (b) Anastassiou, A. G.; Yakali, E. *J. Am. Chem. Soc.* **1971**, *93*, 3803–3805. (c) Anastassiou, A. G.; Yakali, E. *J. Chem. Soc. Chem. Commun.* **1972**, 92–93. (d) Yakali, E. Ph.D. Dissertation; Syracuse University: NY, 1973. (e) Mauksch, M.; Gogonea, V.; Jiao, H.; Schleyer, P. v. R. *Angew. Chem., Int. Ed.* **1998**, *37*, 2395–2397. (f) M. Mauksch, Thesis, University of Erlangen-Nuremberg, 1999, http://www.opus.ub.uni-erlangen.de/opus/volltexte/2007/679/.

(5) Ajami, D.; Oeckler, O.; Simon, A.; Herges, R. *Nature* **2003**, *426*, 819–821.

(6) Castro, C.; Chen, Z.; Wannere, C. S.; Jiao, H.; Karney, W. L.; Mauksch, M.; Puchta, R.; van Eikema Hommes, N. J. R.; Schleyer, P. v. R. *J. Am. Chem. Soc.* **2005**, *127*, 2425–2432.

(7) Castro, C.; Karney, W. L.; Valencia, M. A.; Vu, C. M. H.; Pemberton, R. P. *J. Am. Chem. Soc.* **2005**, *127*, 9704–9705.

(8) Warner, P. M. *J. Org. Chem.* **2006**, *71*, 9271–9282.

(9) (a) Kui, S. C. F.; Huang, J.-S.; Sun, R. W.; Zhu, N.; Che, C. M. *Angew. Chem., Int. Ed.* **2006**, *45*, 4663–4666. (b) Park, J. K.; Yoon, Z. S.; Yoon, M.-C.; Kim, K. S.; Mori, S.; Shin, J.-Y; Osuka, A.; Kim, D. *J. Am. Chem. Soc.* **2008**, *130*, 1824–1825. (c) Pacholska-Dudziak, E.; Skonieczny, J.; Pawlicki, M.; Szterenberg, L.; Ciunik, Z.; Latos-Grazynski, L. *J. Am. Chem. Soc.* **2008**, *130*, 6182–6195. (d) Aihara, J.; Horibe, H. *Org. Biomol. Chem.* **2009**, *7*, 1939–1943.

(10) (a) Schleyer, P. v. R.; Maerker, C.; Dransfeld, A.; Jiao, H.; van Eikema Hommes, N. J. R. *J. Am. Chem. Soc.* **1996**, *118*, 6317–6318. (b) For a review, see: Chen, Z.; Wannere, C. S.; Corminboeuf, C.; Puchta, R.; Schleyer, P. v. R. *Chem. Rev.* **2005**, *105*, 3842–3888.

(11) Martín-Santamaría, S.; Rzepa, H. S. *J. Chem. Soc. Perkin Trans 2* **2000**, 2378–2381.

(12) (a) Fauvel, J.; Flodd, R.; Wilson, R., Eds.; *Möbius and His Band*; Oxford University Press: Oxford, 1993; p 122. (b) Pickover, C. *The Möbius Strip*; Thunder's Mouth Press: New York, 2006.

(13) (a) Fowler, P. W.; Rzepa, H. S. *Phys. Chem. Chem. Phys.* **2006**, *8*, 1775–1777. (b) A closed ribbon embedded in 3D space has twist, T_w, defining in full rotations how much the ribbon twists about its central axis, and writhe, W_r defining how much that axis is contorted in 3D space. Both quantities vary as the ribbon is distorted without breaking, but their sum is a constant, and the linking number is L_k. A system may exchange twist for writhe in 3D space. (c) Adams, C. C. *The Knot Book*; The American Mathematical Society: New York, 2004.

(14) (a) Rzepa, H. S. *Org. Lett.* **2005**, *7*, 4637–4639. (b) Allan, C. S.; Rzepa, H. S. *J. Org. Chem.* **2008**, *73*, 6615–6622.

(15) Rzepa, H. S. *Chem. Commun.* **2005**, 5220–5222.

(16) Gard, M. N.; Reiter, R. C.; Stevenson, C. D. *Org. Lett.* **2004**, *6*, 393–396.

(17) (a) Shimizu, S.; Aratani, N.; Osuka, A. A. *Chem.—Eur. J.* **2006**, *12*, 4909–4918. (b) Stepien, M.; Latos-Grazynski, L.; Sprutta, N.; Chwalisz, P.; Szterenberg, L. *Angew. Chemie, Int. Ed.* **2007**, *46*, 7869–7873. (c) Rzepa, H. S. *Org. Lett.* **2008**, *10*, 949–952. (d) De, S.; Drew, M. G. B.; Rzepa, H. S.; Datta, D. *N. J. Chem.* **2008**, *32*, 1831–1834.

(18) John, R. P.; Park, M.; Moon, D.; Lee, K.; Hong, S.; Zou, Y.; Hong, C. S.; Lah, M. S. *J. Am. Chem. Soc.* **2007**, *129*, 14142–14143. (b) For a reanalysis of this system in terms of L_k, T_w, and W_r, which resolves a difficulty in the original value of the twist, see: Rzepa, H. S. *Inorg. Chem.* **2008**, *47*, 8932–8934.

(19) (a) Dauben, H. J., Jr.; Wilson, J. D.; Laity, J. L. *J. Am. Chem. Soc.,* **1968**, *90*, 811–813, and **1969**, *91*, 1991−1998. (b) Dauben, H. J., Jr.; Wilson, J. D.; Laity, J. L. Diamagnetic Susceptibility Exaltation as a Criterion of Aromaticity. In *Non-Benzenoid Aromatics*; Snyder, J. P., Ed.; Academic Press: New York, 1971; Vol. 2. (c) Schleyer, P. v. R.; Jiao, H. *Pure. Appl. Chem.* **1996**, *68*, 209–218.

(20) (a) All the parent annulene structures were optimized at the B3LYP/6-311+G(d,p) DFT level using the Gaussian 98 and Gaussian 03 programs. The nature of each stationary point was confirmed by vibrational frequency calculations at the B3LYP/6-31G(d) level. Isotropic NICS(0) values were evaluated at the geometrical centers of the carbon rings of the parent annulenes using the deMon−Master NMR program, at the SOS-DFPT level with the Perdew−Wang-91(PW91) exchange correlation functional and the IGLO-III TZ2P basis set as well as at the GIAO-B3LYP/6-31G(d)//B3LYP/6-311+G(d,p) level. The ISE energy evaluations[21] were based on the energy differences between the optimized aromatic and nonaromatic isomers (see Scheme 1) at the B3LYP/6-31G(d) + ZPE level. Magnetic susceptibility exaltations were based on the difference between the magnetic susceptibilities for the same isomers computed at the CSGT-B3LYP/6-31+G*//B3LYP/6-31G(d) level. (b) Frisch, M. J., et al. *Gaussian 03*, revisions C.02 and E.01; Gaussian, Inc.: Wallingford, CT, 2004 and 2008. The full citation is given in the supporting information via the digital repository links. (c) The single point energy computations at the CCSD[T]/dzp level on the B3LYP/

6-311+G(d,p) geometry were performed using the MOLPRO program. . (d) Werner, H.-J., et al. *MOLPRO*, revision 2002.6; University College Cardiff Consultants Ltd.: Cardiff, UK, 2004.

(21) (a) Schleyer, P. v. R.; Pühlhofer, F. *Org. Lett.* **2002**, *4*, 2873–2876. (b) Wannere, C. S.; Schleyer, P. v. R. *Org. Lett.* **2003**, *5*, 865–868. (c) Wannere, C. S.; Moran, D.; Schaad, L. J.; Hess, B. A.; Allinger, N. L.; Schleyer, P. v. R. *Org. Lett.* **2003**, *5*, 2983–2986. (d) Warner, P. M. *J. Org. Chem.* **2006**, *71*, 9271–9282.

(22) (a) White, J. H. *Am. J. Math.*, 1969, *91*, 693−728. (b) Cālugāreanu, G. *Czech Math. J.* **1961**, *11*, 588–625. (c) Fuller, F. *Proc. Natl. Acad. Sci.* **1971**, *68*, 815–819. (d) Pohl, W. *Indiana Univ. Math. J.* **1968**, *17*, 975–985.

(23) An equivalent result is obtained if the p-AOs are to be placed above and below the surface of the ribbon, as illustrated in Figure 1b. This is the model used for **1** as discussed in the text.

(24) Fowler, P. W.; Jenneskens, L. W. *Chem. Phys. Lett.* **2006**, *427*, 221–214.

(25) (a) El-Sagheer, A. H.; Kumar, R.; Findlow, S.; Werner, J. M.; Lane, A. N.; Brown, T. *ChemBioChem.* **2008**, *9*, 50–52. (b) Walba, D. M.; Richards, R. M.; Haltiwanger, R. C. *J. Am. Chem. Soc.* **1982**, *104*, 3219–3221. (c) For an example of a magnetic nuclear ribbon, see: Cador, O.; Gatteschi, D.; Sessoli, L.; Overgaard, F. K.; Barra, A.-L.; Teat, S. J.; Timco, G. A.; Winpenny, R. E. P. *Angew. Chem., Int. Ed.* **2004**, *43*, 5196–5200.

(26) (a) Craig, D. P.; Paddock, N. L. *Nature* **1958**, *181*, 1052–1053. (b) Craig, D. P. *J. Chem. Soc.* **1959**, 997–1001.

(27) Rappaport, S. M.; Rzepa, H. S. *J. Am. Chem. Soc.* **2008**, *130*, 7613–7619.

(28) (a) Becke, A. D.; Edgecombe, K. E. *J. Chem. Phys.* **1990**, *92*, 5397–5403. (b) Savin, A.; Jepsen, O.; Flad, J.; Andersen, O. K.; Preuss, H.; von Schnering, H. G. *Angew. Chem. Int. Ed.* **1992**, *31*, 187–188.

(29) Santos, J. C.; Tiznado, W.; Contreras, R.; Fuentealba, P. *J. Chem. Phys.* **2004**, *120*, 1670–1673.

(30) Kohout, M. DGrid, version 4.3, 2008 was used to compute both ELF_p and $r(r)_p$.

(31) Rzepa, H. S. *Phys. Chem. Chem. Phys.* **2009**, *11*, 1340–1345. This article also addresses the issues that arise in computing the integer L_k from an orbital ribbon at the crossover point for converting a planar system ($L_k = 0$) to one with Möbius topology ($L_k \neq 0$).

(32) (a) Poater, J.; Duran, M.; Sola, M.; Silvi, B. *Chem. Rev.* **2005**, *105*, 3911–3947. (b) Bader, R. F. W. *Atoms in Molecules: a Quantum Theory*; Oxford University Press: Oxford, UK, 1990. (c) Popelier, P. L. A. *Atoms in Molecules: an Introduction*; Prentice- Hall: London, 2000.

(33) (a) To compare performances of various DFT and ab initio levels in predicting most stable [10]annulene conformation, see: King, R. A.; Crawford, D.; Stanton, J. F.; Schaefer, H. F. *J. Am. Chem. Soc.* **1999**, *121*, 10788–10793. (b) This system has been extensively analyzed recently. Castro, C.; Karney, W. L.; McShane, C. M.; Ryan, P.; Pemberton, R. P. *J. Org. Chem.,* **2006**, *71*, 3001–3006. (c) For experimental work on [10]annulene, see: Masamune, S.; Darby, N. *Acc. Chem. Res.* **1972**, *5*, 272–281. Masamune, S.; Hojo, K.; Bigam, G.; Raberstein, D. L. *J. Am. Chem. Soc.* **1971**, *93*, 4966–4968.

(34) Maoche, B.; Gayoso, J.; Ouamerali, O. *Rev. Roum. Chim.* **1984**, *29*, 613.

(35) Chiang, C. C.; Paul, I. C. *J. Am. Chem. Soc.* **1972**, *94*, 4741–4743.

(36) Wannere, C. S.; Sattelmeyer, K. W.; Schaefer, H. F.; Schleyer, P. v. R. *Angew. Chem., Int. Ed.* **2004**, *43*, 4200–4206.

(37) Rzepa, H. S.; Sanderson, N. *Mol. Phys.* **2005**, *103*, 401–405.

(38) Reddy, J. S.; Anand, V. G. *Chem. Commun* **2008**, 1326–1328.

(39) The reported[38] crystal structure of **15** differs from C_{2v} symmetry in the ring bond lengths by ∼0.006 Å (the bond standard errors being ∼0.01 Å). A careful analysis of accurate thermal ellipsoids might distinguish between a single nondynamic structure and one with 50% occupancy of two bond-shifted isomers, but this has not been done. For comparison with possible analyses, B3LYP/6-31G(d) predicts a C_{2v} symmetric minimum, but the KMLYP geometry deviated by ∼0.08 Å from C_{2v} symmetry.

(40) (a) Karney, W. L.; Kastrup, C. J.; Oldfield, S. P.; Rzepa, H. S. *J. Chem. Soc., Perkin Trans 2* **2002**, 388–392. (b) Mauksch, M.; Tsogoeva, S. B. *Eur. J. Org. Chem.* **2008**, 5755–5763.

(41) Mullen, C. *Chem. Rev.* **1984**, *84*, 603–646.

(42) Hoffmann, R.; Schleyer, P. v. R.; Schaefer, H. F. *Angew. Chem., Int. Ed.* **2008**, *74*, 7164–7167.

(43) See, for example: Oth, J. F. M. *Pure Appl. Chem.* **1971**, *25*, 573.

(44) Rzepa, H. S.; Downing, J.; Tonge, A.; Cotterill, F.; Harvey, M. J.; Murray-Rust, Morgan, P.; Day, N. *J. Chem. Inf. Model.* **2008**, *48*, 1571–1581.

JP902176A